Chemical Physics Letters 730 (2019) 521–526

Contents lists available at ScienceDirect

Chemical Physics Letters

journal homepage: www.elsevier.com/locate/cplett

Research paper

Study of structural stability of copper crystal with voids from molecular dynamics simulations

Manash Protim Hazarika, Somendra Nath Chakraborty*

Department of Chemistry, Sikkim University, Gangtok, India

HIGHLIGHTS

- The molecular dynamics simulation work focuses on the melting of copper crystal with voids at 1 bar.
- Several key structural quantities are analysed and the effect of heating in these defective crystals are investigated.
- Results show disappearance of void at a lower temperature and amorphisation of the crystal gradually with heating before melting of the crystal.
- This work provides additional insight in understanding melting of metals with voids.

ARTICLE INFO

Keywords:
Cu melting
Voids
Molecular dynamics
EAM potential

ABSTRACT

We perform molecular dynamics simulations to understand the melting mechanism in Cu crystals (modeled using Embedded Atom Potential) with spherical voids of radii 0.5, 0.6 and 1.0 nm. Along with these systems defect-free Cu and a Cu crystal with layered void is also studied. We analyse crystallinity in these systems using Q_6 bond-orientational order parameter, Lindemann index, radial distribution functions and coordination numbers. At 1 atm, all crystals melt between 1700 and 1800 K and melting temperature decreases with increase in void fraction. It is also found that at 900 K voids disintegrate and become a part of the crystal and between 900 and 1700 K crystals amorphize losing long-range order.

1. Introduction

Melting in crystals is a first-order phase transformation associated with significant changes in density, enthalpy and entropy. Thermodynamic and structural aspects of melting, particularly in bulk samples have been extensively investigated using both experiments and theory [1–3]. One of the most studied aspect of melting has been the test of Lindemann and Born theory [4,5]. Both these theories of homogeneous melting have provided an insightful atomic level description of melting transition. Recently melting studies of solid samples under shock has generated considerable interest [6,7]. Melting of nano-sized clusters of metals have also been studied using molecular dynamics simulations [8–10]. Lately studies of melting in metallic systems with defects, dislocations and grain boundaries are also reported in literature [11–15].

Molecular simulations have played a pivotal role in these studies because atomic level description of melting is unavailable from experiments. In a recent study by Samanta et al. it was showed that melting in crystals can happen through multiple pathways [15]. These competing pathways with multiple metastable states of defects and dislocations lead to the molten state. They illustrated two pathways for melting. In one pathway, melting proceeds via point defects and its diffusion over long distances. In the other pathway, point defects form defect clusters, then dislocations heterogeneously nucleate from these clusters. Authors also contested the applicability of Critical Nucleation Theory for understanding melting transition. Lutsko et al. performed one of the first molecular simulations study of melting in metallic systems. They performed molecular dynamics (MD) simulations of Cu and Si with Embedded Atom Potential containing all kinds of lattice defects. These defects served as nucleation sites for liquid formation. They also observed that with increase in void size melting temperature decreases [11]. From abinitio studies of melting in Argon and Neon Solca et al. showed that melting temperature decreases with void size [16,17]. But after the void reaches a threshold radius, melting temperature does not change. They further state that the temperature at which the critical void melts can be compared with the thermodynamic melting point of the crystals. In another MD study by Agarwal et al. on melting of Argon authors make several important observations [18]. They report that in

* Corresponding author.
E-mail address: snchakraborty@cus.ac.in (S.N. Chakraborty).

https://doi.org/10.1016/j.cplett.2019.06.046
Received 26 March 2019; Received in revised form 11 June 2019; Accepted 17 June 2019
Available online 18 June 2019
0009-2614/

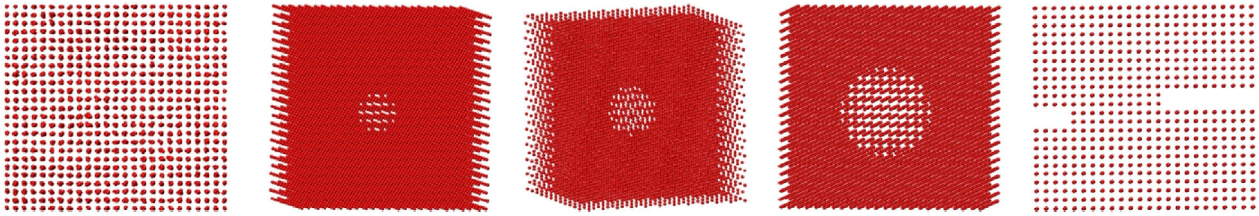

Fig. 1. Initial structure of 12 × 12 × 12 supercell of Cu with and without voids. (left to right – no void, 0.5, 0.6, 1.0 nm and layered void.

crystals without defects mechanical melting happens after thermodynamic melting and this ratio of temperatures is close to 0.8. Mechanical melting point is the limit of mechanical stability. It is located where translational order parameter, number density and energy changes sharply with temperature. In molecular simulations thermodynamic melting point is located using advanced simulation techniques (e.g. perturbation, umbrella sampling etc.) at which free energies of the solid and liquid phases are equal [19]. In most cases, thermodynamic melting temperature obtained from molecular simulations is close to the experimental melting temperature. They also agree with previous simulation studies of Solca et al. [17] that there exist a plateau region where melting temperature does not change with the size of the voids. They further observe that melting temperature depends on the number of atoms removed from the system and not on the shape or location of the void. Similar observations were also made by Puri and Yang [14], who showed that melting temperatures of crystals does not change after a threshold in void size is reached. Their studies performed on Aluminium with different void sizes also show that for smaller voids effect on melting is negligible and melting mechanism is similar to bulk. For voids of size 1 nm^3 melting initiates at those positions where these voids serve as sites for melting. With further increase in void size authors observe structural collapse of the crystal. Kanigel et al. [20] discovered that the bulk melting temperature of Cu depends on the concentration of point defects (namely self-interstitials). Point defects expand the volume of the solid to a critical value at which the mechanical melting transition is produced.

In a recent paper by Bai and Li, melting from nanovoids is studied from MD simulations of LJ particles [21]. They showed void melting is very different from melting in bulk and melting in nano materials. They identified four stages of melting with two local melting temperatures which depend on void size. They also observe a plateaue in melting transition temeperature with increase in fraction of void. Unlike previous studies Bai and Li report this plateau as a function of void fraction and not as a function of radii. They further show that stability of a void is determined by the solid-liquid interfacial energy and elastic energy. Similar to these observations, Li and Qi [22] in a recent study show that melting is decided by the differences in interfacial energy between solid-vapour, solid-liquid and liquid-vapor. Interestingly they observed that if $\Delta\gamma$ ($\Delta\gamma = \Delta\gamma_{sv} - (\Delta\gamma_{sl} + \Delta\gamma_{lv})$) is negative void shrinks and disappears only when the matrix melts. This happens in crystals of Si, whereas in crystals of Pd where $\Delta\gamma$ is positive void melts first and then the crystal melts. They thus identified these two types of melting mechanism namely – Nucleating (NM in Pd) and Non-nucleating (NNM in Si) from interfacial tension values.

Our study is particularly motivated by this work of Li and Qi where authors have unified melting via nucleation and non-nucleation mechanism using interfacial tension calculations [22]. Authors show that difference in interfacial tension decides the mechanism of melting. Our study focusses on understanding the loss of structure in defect free and defective Cu crystal and test whether it melts NM or NNM way. We create different size of spherical voids anda layered void in the crystal to analyse their effect. Void fractions in our study is varied from 1 to 7%. Our conclusions are based on the behaviour of structural quantities during heating of the crystal.

2. Computational details

Molecular dynamics simulations of bulk Cu with three spherical and one layered defect was simulated at 1 bar and at different temperatures. Bulk defect free FCC Cu in 12 × 12 × 12 unit cell containing 6912 atoms was simulated from 300 K to 2000 K at an interval of 200 K. At each temperature defect free Cu system was equilibrated for 5 ns.At 300 K two different types of void was created in the bulk crystal, namely – spherical and layered. In spherical voids, Cu atoms within radii 0.5, 0.6 and 1.0 nm relative to center of the bulk Cu crystal is removed. In layered void, similar number of Cu atoms removed in 1 nm spherical void crystal was also removed from one portion of the Cu crystal. All these systems were then independently equilibrated at each temperature from 300 to 2000 K at an interval of 200 K for 5 ns. At 300 K, initial configuration for void free crystal was FCC copper and for void systems were FCC copper with artificially created voids in them. All simulations were initiated with the last equilibrated configuration obtained from the previous temperature. All simulations were performed using standard cubic periodic boundary conditions. Fig. 1 shows the snapshot of defect free and defective Cu with spherical and layered void. Analyses was performed from 5000 configurations collected after 5 ns at an interval of 0.2 ps. Here we have used the originally developed Embedded Atom Potential for Cu in all the simulations [23]. This potential was first proposed by Dow and Baskes in 1987 and it has been mostly used for the simulation of metallic systems like Cu, Ni, Pb etc. EAM is based on density functional theory (DFT). In this method each atom is embedded in a host electron gas generated by all surrounding atoms. The amount of energy needed to put one atom into the electron gas of a given density is called the embedding function, which considers many atom effects. In a simulation, the potential energy of an atom, i, is given by-

$$E_i = F_\alpha\left(\sum_{i\neq j}\rho_\beta(r_{ij}) + \frac{1}{2}\sum_{i\neq j}\phi_{\alpha\beta}(r_{ij})\right) \quad (1)$$

where r_{ij} is the distance between atoms i and j , $\phi_{\alpha\beta}$ is a pair-wise potential function, ρ_β is the contribution to the electron charge density from atom j of type β at the location of atom i, and F is an embedding function that represents the energy needed to put atom i of type αinto the electron cloud.This potential for Cu correctly reproduce the thermodynamic melting temperature of Cu crystal (T_m = 1340 K) [24] and its other properties [25].

LAMMPS MD software was used for all the simulations. Simulations were performed with cubic periodic boundary conditions under isothermal-isobaric conditions. We have employed Nosé-Hoover barostat to control the pressure fluctuation during simulation. Nosé-Hoover barostat was described by Martyna et al. [26] which is based on constant temperature method proposed by Anderson [27]. To control the temperature we employ Nosé-Hoover thermostat, introduced by Nosé [28] and subsequently developed by Hoover [29]. We use Verlet [30] algorithm to integrate the Newtonian equation of motion with an integration time-step of 2 fs.

We analyse the equilibrated configurations using four structural quantities – Lindemann index, Q_6 bond orientational order parameter, radial distribution function and coordination number. Structural

melting temperature is often defined by root mean square bond fluctuation, called Lindemann index δ[9]. The Lindemann index of each atom and of the entire bulk system is calculated using [31].

$$\delta_i = \frac{1}{N-1}\sum_{j\neq i}\frac{\sqrt{<r_{ij}^2>_T - <r_{ij}>_T^2}}{<r_{ij}>_T} \quad (2)$$

$$\delta = \sum_i \delta_i \quad (3)$$

where N is the number of atoms. δ_i and δ are the Lindemann indices of i th atom and bulk respectively, r_{ij} is the distance between i th atom and j th atom.

Bond orientational order parameters were introduced by Steinhardt [32]. These spherical harmonics based order parameters measures the degree of crystallinity of the solid [33]. For each atom, Q_6 bond orientation order parameter is calculated in the following way [34].

$$\overline{Y}_{lm} = \frac{1}{nnn}\sum_{j=i}^{nnn} Y_{lm}(\theta(r_{ij}), \phi(r_{ij})) \quad (4)$$

$$Q_l = \sqrt{\frac{4\Pi}{2l+1}\sum_{m=-l}^{m=l}\overline{Y}_{lm}\overline{Y}_{lm}^*} \quad (5)$$

The summation over the *nnn* stands for nearest neighbor of the central atom. θ and ϕ are the standard spherical polar angles. Q_l(here l = 6) in the second equation is rotationally invarient scalar quantity [34]. Here the nearest neighbors of a central Cu atom is collected based on a cut-off. First minimum of the Radial Distribution Fuction (RDF) at each temperature was used as the cut-off for the choice of nearest neighbor of Cu atoms. The pair correlation function or the radial distribution function $g(r)$ is a crucial structural property of a liquid and is defined as the ratio of the relative probabilities of finding two particles separated by a distance r in a liquid and in an ideal gas. Average coordination of molecules (n) were calculated employing the temperature dependent spherical cut-off.

3. Results

All five systems were studied under isothermal-isobaric conditions at 1 bar. Results shown here are for all the systems at 900 K and onwards. Quantities like Enthalpy, Density and Diffusivity are presented in Supplementary section and not discussed here.

Fig. 2 shows the Lindemann index and Q_6 bond-orientational order parameter as a function of temperature. Here Q_6 is the global quantity summed and averaged over all local Q_6 of Cu atoms lying within the cut-off. Both these quantities change sharply as the crystal melts. Lindemann index is a measure of mean square displacement of particles. It increases linearly with temperature, and changes sharply between 1740 and 1780 K for defect free Cu and defective Cu with the smallest spherical void. For rest of the systems, this quantity increases sharply between 1600 and 1700 K. Moreover overall magnitude of lindemann index for 0.6, 1.0 nm and layered void system is almost 10% higher than defect free Cu and Cu with the 0.5 nm spherical void. Bond orientational order parameter decreases linearly with temperature. Similar to lindemann index for defect free Cu and defective Cu with the smallest spherical void melting occurs between 1740 ad 1780 K and for rest of the systems happen between 1600 and 1700 K. Also similar to lindemann magnitude of Q_6 of 0.6, 1.0 nm and layered void system is almost 10% higher than defect free Cu and Cu with 0.5 nm spherical void. Both these quantities are a measure of crystallinity and mechanical stability of the system. With increase in temperature crystallinity decreases and at melting when the whole system melts long range order disappears completely. Interestingly for 0.6, 1.0 nm and layered void degree of crystallinity in the solid is always less than that of defect free Cu and Cu with smallest void.

Radial distribution functions of defect free and defective Cu is shown in Fig. 3. Loss of long range order in the crystal is observed from the disappearance of peaks beyond 0.6 nm and broadening of all peaks. In defect free Cu and Cu with void of 0.5 nm melting completes by 1780 K. In defective Cu with 0.6 and 1.0 nm spherical voids liquid appears earlier at 1700 K. Moreover with decrease in temperature for all the systems crystallinity decreases with temperature and long range order starts disappearing from 1000 K onwards (crystal with 0.6 and 1.0 nm void losing it before defect free and defective crystal with 0.5 nm void)). For the layered system RDF shown in Fig. 4 is similar to the spherical 1.0 nm void system. Liquid appears at 1700 K and the long range pair correlations disappear with increase in temperature.Fig. 2 and 3 shows the overall melting in all the crystals. All these systems melt between 1500 and 1800 K. To assess structural stability of atoms at the vapour-solid interface Q_6 and coordination number of these atoms were investigated at 900 K. Cu Atoms closest to the center of the void (for sphericalvoids) were chosen as the first layer of the vapour-solid interface. The coordination numbers of all these atoms were less than 12. Thereafter for the layered void system atoms with coordinations less than 12 were identified as atoms at vapour-solid interface. For all the defective systems Q_6 and coordination number as a function of time is plotted in Fig. 5. Here Q_6 and n was averaged for all atoms lying within the cut-off. These two quantities for atoms at the vapor-liquid interface was then compared with the rest of the Cu atoms. Fig. 5(a) and (b) shows the coordination number and Q_6 order parameter for atoms lying at the vapour-liquid interface of the void. Fig. 5(c) and (d) shows the coordination number and Q_6 for rest of the atoms which are not a part of the first layer of the void. Interestingly, within first 10 to 15 ps both coordination number and Q_6 stabilises. Atoms which did not have enough of Cu atoms surrounding them slowly picks up in coordination. In these systems degree of crystallinity also picks up marginally. Fig. 5(a) and (b) clearly shows the immediate collapse of the void. For the rest of the atoms also situation is somewhat similar where coordination number stabilises around 12 and there is a marginal decrease in the crystallinity. It is important to note that all of it happens at 900 K much before the crystal actually melts.This study was performed to compare the stability of our void system with results obtained by Bai and Li [21]. Our picture of void collapse compares well with Bai and Li results.

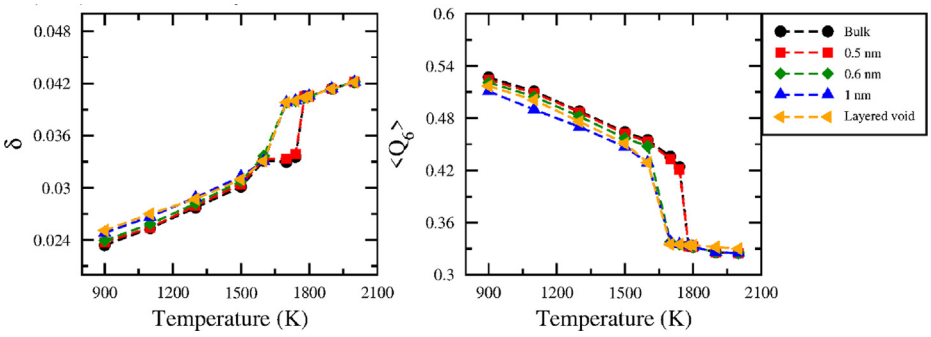

Fig. 2. Lindemann Index and Q_6 bond-orientational order parameter as a function of temperature.

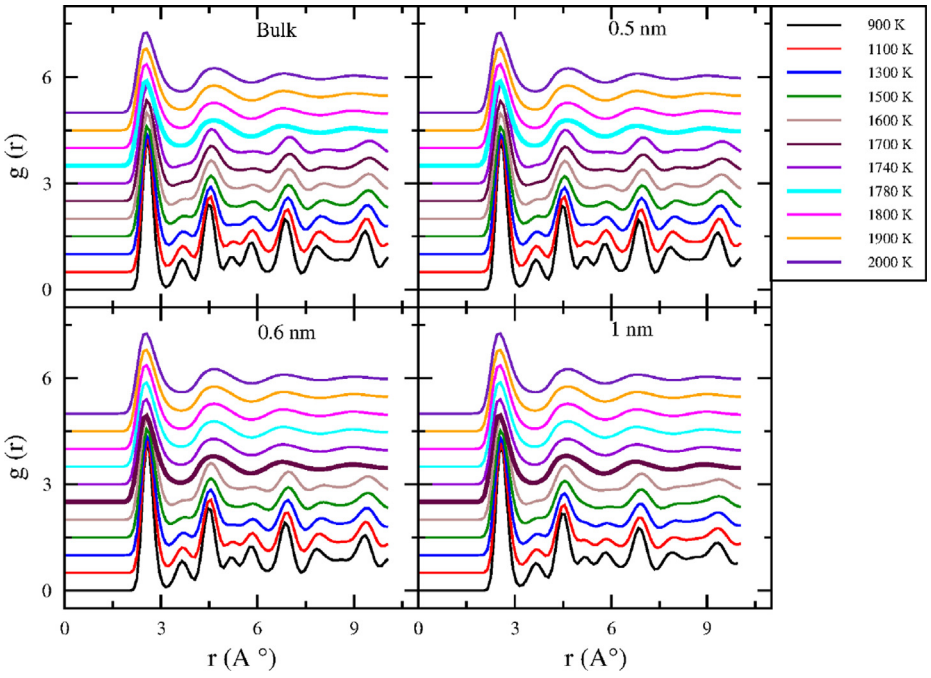

Fig. 3. Radial distribution functions of defect free bulk Cu and Cu with 0.5, 0.6 and 1.0 nm spherical void. Liquid appears at 1780 K for bulk and 0,5 nm spherical void (bold cyan) and at 1780 K for 0.6 and 1.0 nm spherical void (bold maroon). (For interpretation of the references to colour in this figure legend, the reader is referred to the web version of this article.)

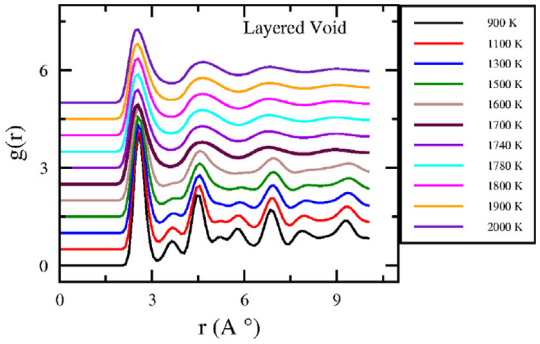

Fig. 4. Radial distribution functions of Cu with layered void. Liquid appears at 1700 K (bold maroon). (For interpretation of the references to colour in this figure legend, the reader is referred to the web version of this article.)

Fig. 6 shows the orientational ordering in 12 and 13 coordinated atoms of all Cu systems at different temperatures. It was estimated for all systems, 12 and 13 coordinations constitute almost 90 percent of Cu atoms (Fraction estimates are provided in Supplementary Section) till melting occurs.Crystallinity in 12 and 13 coordinated Cu atoms are followed with increase in temperature. The peak at highest Q_6 appears at 900 K and the lowest Q_6 peak first appears around 1700 K. Similar to previous results voids greater than 0.6 nm melts earlier than 0.5 nm and defect free systems. For the defect free and 0.5 nm void system all coordinations lose crystallinity by 1780 K. But for 0.6 nm, 1.0 nm and the layered void crystallinity is completely lost at 1700 K. But for all the coordinations peaks broaden and shift on heating which shows that crystallinity is lost gradually. As observed earlier with the disappearance of the larger void at 900 K, local coordinations with heating gradually loses their structure but the crystal does not collapse abruptly. When correlations at a short distance disappear then only the crystal melts.

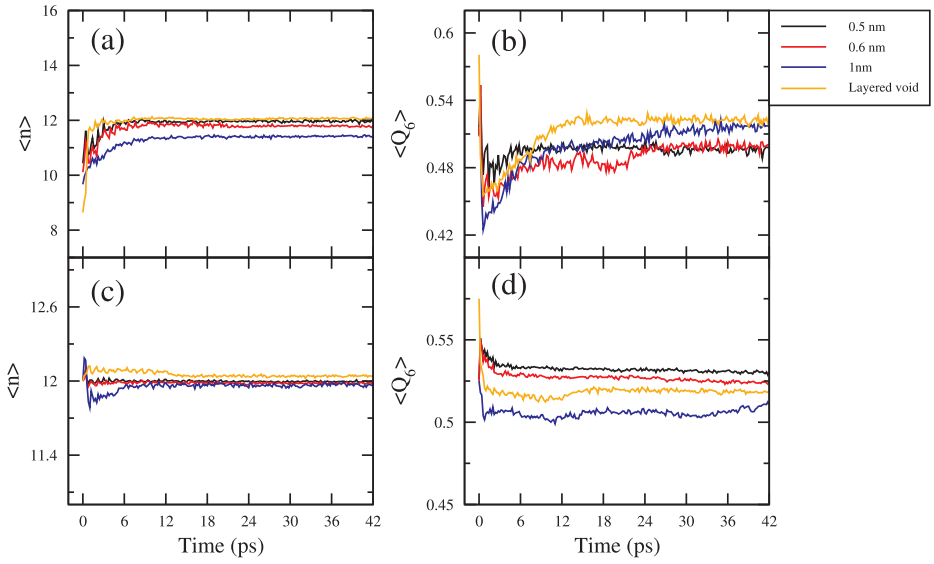

Fig. 5. Coordination number and Q_6 order parameter of atoms at the solid-vapor interface of the void (a) and (b) and of rest of the atoms (c) and (d) at 900 K.

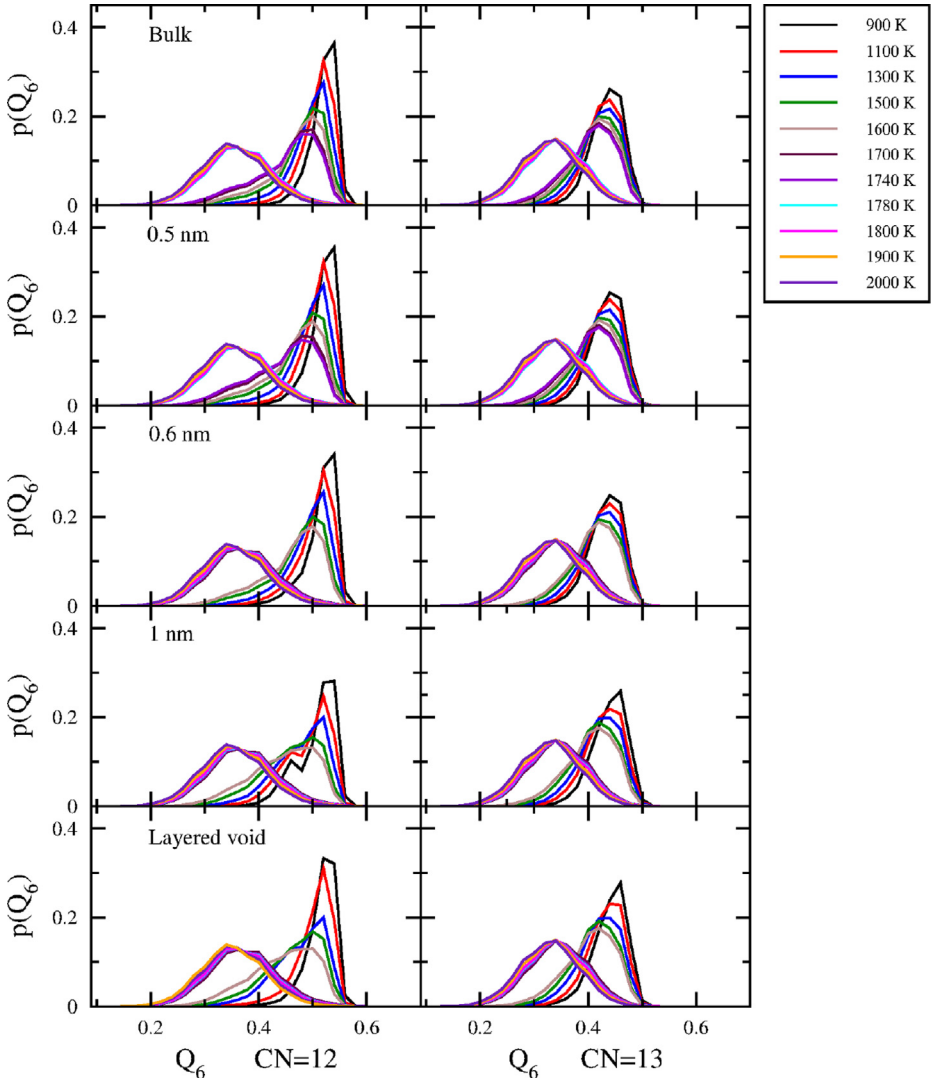

Fig. 6. Q_6 order parameter distribution of 12 and 13 coordinated Cu atoms for all systems at all temperatures.

4. Conclusion

From our molecular dynamics simulations we observe few important aspects of melting. Melting temperature of void system depends on the volume fraction of void which is similar to results earlier obtained by Li et al. [21]. As observed by Solca et al. we also find no change in melting temperature for voids above 0.6 nm [17]. Compared to observations made by Agarwal et al. we find melting depends on void fraction (number of atoms removed) and not on the shape of the void [18]. In our systems melting of layered void and spherical void of 1 nm occurs similarly and at same temperature (here similar number of Cu atoms are removed from the system). From unified theory of NM and NNM defective Cu ($\Delta\gamma$ is positive) should melt in the following way – void collapses produces a liquid and then the matrix melts [22]. We also observe spherical voids to collapse because the solid-vapour surface tension is not enough for this interface to be stable. But once this happens we find over the next 500–600 K solid amorphises with the gradual loss of long-range order and crystallinity. Unlike previous observations made by Bai and Li and Li and Qui where they show the matrix is crystalline after collapse of void we note that the matrix is not crystalline but it gradually amorphises with heating. As temperature is increased further, thermal fluctuations increase and overall long range ordering of the crystal starts disappearing. Finally when correlations at short distances disappear crystal melts. And as explained from Lindemann Index, when fluctutations reach a threshold value, crystal collapses to liquid. This kind of structural melting was also observed earlier by Puri et al. [14].

Declaration of Competing Interest

The authors declared that there is no competing interest.

Acknowledgements

MPH would like to thank Sikkim University for the fellowship. SNC would like to thank Sikkim University for providing the computational facilities to perform the simulations.

Appendix A. Supplementary data

Supplementary data associated with this article can be found, in the online version, at https://doi.org/10.1016/j.cplett.2019.06.046.

References

[1] G.R. Gathers, Int. J. Thermophys. 4 (1983) 209–226.
[2] A.B. Belonoshko, R. Ahuja, O. Eriksson, B. Johansson, Phys. Rev. B 61 (2000) 3838.
[3] S.A. Etesami, E. Asadi, J. Phys. Chem. Solids 112 (2018) 61–72.
[4] F.A. Lindemann, Z. Phys. 11 (1910) 609.

[5] M. Born, J. Chem. Phys. 7 (1939) 591–603.
[6] A.M. He, S. Duan, P. Jian-Li Shao, C. Qin Wang, J. Appl. Phys. 112 (2012) 074116.
[7] Y. Ju, Q. Zhang, Z. Gong, G. Ji, L. Zhou, J. Appl. Phys. 114 (2013) 093507.
[8] L. Wang, Y. Zhang, X. Bian, Y. Chen, Phys. Lett. A 310 (2003) 197–202.
[9] H.H. Kart, H. Yildirim, S.O. Kart, T. Çağin, Mater. Chem. Phys. 147 (2014) 204–212.
[10] J. Zhang, X. Wang, Y. Zhu, T. Shi, Z. Tang, M. Li, G. Liao, Comput. Mater. Sci. 143 (2018) 248–254.
[11] J.F. Lutsko, D. Wolf, S.R. Phillpot, S. Yip, Phys. Rev. B 40 (1989) 2841.
[12] P. Heino, H. Häkkinen, K. Kaski, Phys. Rev. B 58 (1998) 641.
[13] V. Sorkin, E. Polturak, J. Adler, Phys. Rev. B 68 (2003) 174102.
[14] P. Puri, V. Yang, J. Nanopart. Res. 11 (2009) 1117–1127.
[15] A. Samanta, Mark E. Tuckerman, Tang-Qing Yu, E. Weinan, Science 346 (2014) 729–732.
[16] J. Solca, A.J. Dyson, G. Steinebrunner, B. Kirchner, H. Huber, Chem. Phys. 224 (1997) 253–261.
[17] J. Solca, A.J. Dyson, G. Steinebrunner, B. Kirchner, H. Huber, J. Chem. Phys. 108 (1998) 4107–4111.
[18] P.M. Agrawal, B.M. Rice, D.L. Thompson, J. Chem. Phys. 118 (2003) 9680–9688.
[19] C.-S. Zha, R. Boheler, J. Chem. Phys. 85 (1986) 1034–1036.
[20] A. Kanigel, J. Adler, E. Polturak, Int. J. Mod. Phys. C 12 (2001) 727–737.
[21] X.M. Bai, M. Li, Nano Lett. 6 (2006) 2284–2289.
[22] S. Li, W. Qi, J. Phys. Chem. C 119 (2015) 6843–6851.
[23] M.S. Daw, M.I. Baskes, Phys. Rev. B 29 (1984) 6443.
[24] M.S. Daw, S.M. Foiles, M.I. Baskes, Mater. Sci. Rep. 9 (1993) 251–310.
[25] B. Sadigh, G. Grimvall, Phys. Rev. B 54 (1996) 15742.
[26] G.J. Martyna, D.J. Tobias, M.L. Klein, J. Chem. Phys. 101 (1994) 4177–4189.
[27] H.C. Andersen, J. Chem. Phys. 72 (1980) 2384–2393.
[28] S. Nosé, J. Chem. Phys. 81 (1984) 511–519.
[29] W.G. Hoover, Phys. Rev. A 31 (1985) 1695.
[30] L. Verlet, Phys. Rev. 159 (1967) 98.
[31] F. Ding, K. Bolton, A. Rosén, Eur. Phys. J. D-Atom. Mol. Opt. Plasma Phys. 34 (2005) 275–277.
[32] P.J. Steinhardt, D.R. Nelson, M. Ronchetti, Phys. Rev. B 28 (1983) 784.
[33] W. Lechner, C. Dellago, J. Chem. Phys. 129 (2008) 114707.
[34] <https://lammps.sandia.gov/doc/compute_orientorder_atom.html>.